Optimizing a Waveguide-Based Sandwich Immunoassay for Tumor Biomarkers: Evaluating Fluorescent Labels and Functional Surfaces

Harshini Mukundan,[†] Hongzhi Xie,[†] Aaron S. Anderson,[†] W. Kevin Grace,[†] John E. Shively,[‡] and Basil I. Swanson*,[†]

MS: J567, Physical Chemistry and Applied Spectroscopy, Los Alamos National Laboratory, Los Alamos, New Mexico 87545, and Beckman Research Institute, City of Hope, 1450 East Duarte Road, Duarte, California 91010. Received July 8, 2008; Revised Manuscript Received November 25, 2008

The sensor team at the Los Alamos National Laboratory has developed a waveguide-based optical biosensor for the detection of biomarkers associated with disease. We have previously demonstrated the application of this technology to the sensitive detection of carcinoembryonic antigen in serum and nipple aspirate fluid from breast cancer patients. In this publication, we report improvements to this technology that will facilitate transition to a point-of-care diagnostic system and/or robust research tool. The first improvement involved replacing phospholipid bilayers used for waveguide functionalization with self-assembled monolayers. These thin films are stable, specific, and robust silane-based surfaces that reduce nonspecific binding and enhance the signal to background ratio. Second, we have explored four different fluorescent labeling paradigms to determine the optimal procedure for use in the assay. Labeling the detector antibody with an organic dye (AlexaFluor 647) in the hinge region allows for unusual signal enhancement with repeat excitation (at 635 nm) in our assay format, thereby facilitating a better signal resolution at lower concentrations of the antigen. We have also labeled the detector antibody with photostable quantum dots through either the amine groups of lysine (Fc, NH) or using a histidine tag in the hinge region of the antibody (Hinge, H). Both labeling strategies allow for acceptable signal resolution, but quantum dots show much greater resistance to photobleaching than organic dyes.

INTRODUCTION

Breast cancer affects 200 000 women annually in the United States. The probability of survival is much higher with early diagnosis (95%) compared to metastatic disease (26%) (*1*). Current diagnostic techniques are, however, unsatisfactory when applied to early detection. For example, mammography can detect the tumor only when palpable, suffers from high false positive and negative rates, and requires confirmatory invasive biopsies as a consequence. In addition, it cannot be used on women less than 40 years of age because of intrinsically denser breasts in that population (*2*). Other methods are also either expensive (e.g., magnetic resonance imaging) or are associated with nonspecific results (standard immunoassays) (*3*). Thus, there is a need for a sensitive, specific, quantitative, rapid, and noninvasive diagnostic for breast cancer.

Certain "biomarkers" are differentially expressed in cancer, typically very early in disease onset, and can potentially be used for detection. Since no single biomarker can effectively predict all stages of cancer, detection of a suite of these molecules is a requisite of any diagnostic strategy that utilizes them. However, current immunoassay techniques cannot accomplish this in complex, small-volume patient samples. Therefore, the American Society for Clinical Oncology does not currently recommend these markers for the early detection of breast cancer (*4*).

The sensor team at the Los Alamos National Laboratory has developed a waveguide-based optical biosensor for the sensitive detection of such markers in a sandwich immunoassay format. The optical properties and assay procedures have been outlined elsewhere (*5*). Briefly, a sandwich immunoassay using a fluorescently labeled detector antibody is performed on the functionalized surface of single-mode planar optical waveguides. Only fluorescent molecules within the evanescent field of the waveguide (0−250 nm from the surface) are excited, facilitating optical separation of surface-bound entities from solution contaminants. This spatial filtering minimizes the background fluorescence associated with complex biological samples such as blood and sputum. We have previously demonstrated the application of this technology to the sensitive detection of breast cancer (unpublished data) (*6*), influenza viruses (*7*), and *Bacillus anthracis* protective antigen (*5*). We have successfully adapted the optical biosensor to the detection of carcinoembryonic antigen (CEA), a breast cancer biomarker in serum and nipple aspirate fluid from patients with abnormal mammograms (unpublished data) (*6*). CEA was detected in a small cohort of patient samples with excellent sensitivity (limit of detection = <0.5 pM), specificity (low nonspecific binding or false results), and speed (15 min). We have assessed the reproducibility of our assay by two different approaches. Repeat measurements were made with 25 pM human CEA on the same waveguide as a measure of intra-assay variability. The signal observed with each measurement was completely eliminated by photobleaching before subsequent measurements were made. The waveguide background was low (∼16 relative fluorescence units (RFU)) with a standard deviation of 3 between measurements. 25 pM CEA yielded, on average, 1046 RFU with a standard deviation of 119 between measurements. We have also assayed for interassay variability by measuring CEA concentrations in a human patient sample in 4 different waveguides in entirely different experiments. Although the raw values for background and signal differ among waveguides, the extrapolated CEA concentration (based on an internal human purified CEA

* To whom all correspondence is addressed. MS J567, C-PCS, C-Division, Los Alamos National Laboratory, Los Alamos, New Mexico 87545, basil@lanl.gov, (505)-667-5814(phone), (505)-667-0440 (Fax).

[†] Los Alamos National Laboratory.

[‡] City of Hope.

10.1021/bc800283e CCC: $40.75
Published on Web 01/27/2009

standard) was 78 pM ($n = 4$ repeats) with a standard deviation of <1.5. These numbers establish both the inter- and intra-assay reproducibility of our waveguide-based assay for CEA (*5*). However, our waveguide assay still required optimization to make it more amenable for use in clinical or research setting. For instance, phospholipid bilayers (PLBs) used in the initial demonstration for waveguide surface functionalization, are neither robust nor stable, and allow nonspecific interactions in complex biological samples. Our team has developed alternative functional surfaces that overcome these disadvantages. Silane-based self-assembled monolayers (SAMs) are robust (can be washed with detergents) and stable (>300 days in air), effectively resist nonspecific interactions, and are potentially regenerable (*8*). The present manuscript demonstrates the superior performance of SAMs (in comparison with PLBs) when applied to the detection of CEA.

In our initial demonstration of the CEA assay, the detector antibody was labeled with an organic dye (AlexaFluor 647, AF647) in the Fc region (primary, NH labeling) using the NH groups on the lysine residues. The current study compares this strategy to one where the antibody is labeled with AF647 in the hinge region (H labeling) using a histidine tag. In addition to organic dyes, we have also analyzed the use of photostable quantum dots (QDs) as the fluorescent label. QDs have been extensively researched as fluorescence reporters or probes for several biological applications (*9*). They consist of nanometer-scale atom clusters with a semiconductor core and shell and an amphiphilic polymer coating (*10*) that provides a protective, water-soluble surface that can be differentially modified. QDs show a direct, predictable relationship between their physical size and the energy of the exciton (and, therefore, the wavelength of emitted fluorescence). This "tuneability" has allowed for the development of a series of QDs that have common excitation profiles but different fluorescent emission maxima. Exploiting this property, one can potentially envision a multiplex detection format using QDs that emit at different wavelengths. In addition, QDs exhibit excellent brightness and much greater photostability than traditional organic fluorophores (*9*). This makes long-term imaging/excitation possible under conditions that would lead to the photoinduced deterioration (photobleaching) of other types of fluorophores. These features have facilitated the use of QDs in several bioapplications such as immunofluorescence assays, live cell imaging, biotechnology detection, single molecule biophysics, and in vivo animal imaging (*11*−*13*). NH-and H-labeling with both QDs and organic dyes were evaluated in the current study. NH labeling has been shown to sometimes compromise antigen binding activity of the antibody. Therefore, we chose to evaluate two different labeling protocols and determine the one that offered the best sensitivity.

EXPERIMENTAL PROCEDURES

Materials. Purified CEA and antibodies (T84.1, capture and T84.66, detector) were obtained from our collaborators at the City of Hope. These antibodies were selected by epitope mapping and therefore form an effective sandwich by binding orthogonal epitopes of CEA (unpublished data) (*6*). Amino-functionalized QD (655 nm, QD655), Qdot655 ITK carboxyl quantum dots, and AF647-*N*-hydroxysuccinimide (NHS) ester labeling kits were purchased from Invitrogen. Biotinylation, protein estimation, and electrophoresis reagents were obtained from Pierce. Tri-*n*-octylphosphine oxide (TOPO) and tri-*n*-octylphosphorine (TOP) capped CdSe/ZnS core/shell QDs were a generous gift from Dr. S. Jeong (Los Alamos National Laboratory) (*14, 15*).

Gel filtration columns and spin filters were from Harvard Apparatus. Buffers, chemicals, immunoblot materials, and other components were purchased from Sigma Aldrich or Fisher Scientific unless otherwise specified. Waveguides were obtained from nGimat, Atlanta, GA. 1,2-Dioleoyl-*sn*-glycero-3-phosphocholine (DOPC) and 1,2-dioleoyl-*sn*-glycero-3-phosphoethanolamine-*N*-(cap biotinyl) (sodium salt) were purchased from Avanti Polar Lipids. Materials required for SAM preparation are listed in detail elsewhere (*8*).

Methods. *Biotinylation of the Capture Antibody.* The capture antibody (2 mg/ml, 500 μL) was incubated with Sulfo-NHS biotin (10 mM, 20 molar excess) for 1 h at room temperature (RT) on a rotator. Macro Spin gel filtration columns (molecular weight cutoff (MWCO) 100 kD, 150 μL capacity) were hydrated for 2 h with PBS, and the biotinylated antibody was separated from free-biotin by centrifugation in the hydrated columns for 5 min. The extent of biotinylation was determined using an EZ Biotin Quantitation Kit (Pierce) that measures the degree of biotinylation using 4′-hydroxyazobenzene-2-carboxylic acid. Protein concentration was determined by measuring absorbance of the conjugate at 280 nm using bovine serum albumin (BSA) as the standard.

Functionality of the biotinylated antibody (i.e., ability to bind antigen) was assessed by immunoblot analysis. For this, CEA (1 nM, 3 μL) was blotted on nitrocellulose filter paper and allowed to air-dry. The paper was subsequently blocked with fish gelatin (4.5% v/v solution in PBS) for 2 h at RT and probed overnight at 4 °C with the biotinylated antibody. Unbound antibody was removed by washing with PBS/Tween-20 (0.1% v/v, 3×, 1 min each) followed by PBS (4×, 1 min each). The blot was then incubated with a secondary antibody (goat−anti-mouse labeled with alkaline phosphatase, 0.001 mg/mL, 2 mL, 1 h at RT). Again, unbound antibody was removed by washing and specific staining detected with NBT-BCIP (one-step alkaline phosphatase substrate). Unlabeled antibody was used as the positive control and PBS-0.5% BSA as the negative. The same protocol was also used for the evaluation of the fluorescently labeled detector antibodies (see below).

Biotinylation of the capture antibody (i.e., incorporation of biotin on the antibody) was also assessed by immunoblot. One nanomolar antibody was blotted on nitrocellulose filter paper. Following blocking, the blot was probed using streptavidin labeled with alkaline phosphatase (0.001 mg/mL in PBS, 2 mL) for 1 h at RT. Unbound antibody was removed by washing, and the blot was developed as described earlier. Unlabeled antibody was used as the negative control and sulfo-NHS-biotin as the positive control.

Fluorescent Labeling of the Detector Antibody. Multiple strategies were used for generating fluorescent detector bioconjugates. In each case, protein concentration was measured by determining absorbance at 280 nm using bovine serum albumin (BSA) as standard. Functionality of the labeled antibody was evaluated by immunoblot analysis (as outlined earlier). Labeling was verified, where applicable, by gel electrophoresis. Both agarose and polyacrylamide (PAGE) gel electrophoresis techniques were employed.

Primary Labeling of Detector Antibody with AF647 (T84.66-NH-AF647). An AF647-NHS ester labeling kit (catalogue #A20173, Invitrogen) was used, and the reaction was carried out according to the manufacturer's recommendation. Briefly, the antibody (2 mg/mL, 500 μL) was reacted with AF647-NHS ester in the dark for 1 h at RT on a rotator. Labeled protein was separated from free dye by gel filtration (G-25, Sephadex). Degree of labeling was determined by UV/vis spectroscopy to be 4 mol of dye per mole of protein based on the corrected ratio of absorbance at 650 and 280 nm, respectively.

Hinge Labeling of Detector Antibody with AF647 (T84.66-H-AF647). Detector antibody (8 mg/mL, 500 μL) in PBS, pH 8.0, was reacted with 20 mM tris(2-carboxylethyl) phosphine (TCEP) (400 nmol, 30-fold molar excess) at 37 °C for 2 h under

argon. The mixture was purified by spin filtration (G-25, Sephadex) and then reacted with a 50 molar excess of AF647-maleimide in PBS at 37 °C for 2 h under argon on a rotator. The reaction mixture was again purified by G-25 spin filtration (MWCO 100 kD), and labeled protein was collected. Protein reduction was confirmed by nonreducing gel electrophoresis.

NH Labeling of Detector Antibody with QD (T84.66-NH-QD655). Carboxyl-coated QD655 stock solution (8 μM, 20 μL) was blended in borate buffer (25 mM, pH 7.3) and mixed with the antibody (47 μM, 10 μL). *N*-Ethyl-*N*′-dimethylaminopropylcarbodiimide hydrochloride (EDC, 100 mM, 2.4 μL) was added to this reaction mixture and gently stirred for 2 h at RT. The reaction was quenched by addition of borate buffer (50 mM, 100 μL, pH 9.0) and further incubated for 2 h at RT.

Free and conjugated QDs were visualized by sodium dodecyl sulfate (SDS)-PAGE followed by UV illumination at 366 nm. Proteins were stained with GelCode (blue) reagent. The conjugate was separated by spin filtration (membrane MWCO 100 kDa) followed by at least five exchanges with borate buffer (50 mM, pH 8.5). Absorbance of QD655 was measured to calculate its concentration ($\varepsilon_{638} = 8 \times 10^5$ M^{-1} cm^{-1}). The molar ratio of antibody to QD in the conjugate was 3:1.

Hinge Labeling of Detector Antibody with QD625 (T84.66-H-QD625). [TOP/TOPO]-capped CdSe/ZnS core/shell quantum dots with an emission maximum at 625 nm were used to prepare dihydrolipoic acid (DHLA)-coated QDs (*16*). DHLA was freshly prepared from α-lipoic acid by sodium borohydride reduction (*17*). DHLA-QD625 (1 μM, 100 μL) was diluted with borate buffer (25 mM at pH 9.0, 78 μL), mixed with His_6-anti-CEA antibody (18 μM, 22 μL), and incubated overnight at 4 °C. Conjugation was verified by running the His_6-anti-CEA-DHLA-QD625 on native polyacrylamide (4−15% gradient) and agarose (1%) gels. This confirmed the absence of free QDs in the conjugate. Absorbance of the conjugate was used to determine QD625 concentration ($\varepsilon_{605} = 4.5 \times 10^5$ M^{-1} cm^{-1}). Antibody concentration was determined by the Bicinchoninic acid assay (BCA) using BSA as standard. The average number of antibodies per QD was about 4.

Preparation of the Waveguides and Coating with Sensing Film(s). Single-mode planar optical waveguides consisting of a polished fused silica substrate (lower refractive index) coated with silicon oxy nitride (SiON*x*, high refractive index) with a 10 nm coating of SiO_2 (lower refractive index, which allows the functionalization of the waveguide surface) were used. Waveguides and glass coverslips were cleaned by sonication in chloroform and ethanol (5 min each), followed by exposure to UV-light and ozone (40 min). The cleaned surfaces were functionalized using either PLBs or SAMs.

The preparation of biotinylated (1%) unilamellar vesicles (PLBs) by sonication has been previously described (*5*). Briefly, thin films of DOPC (5 mM stock in $CHCl_3$, 50 μL) with 1% cap biotinyl (v/v, sodium salt, 5 mM stock in $CHCl_3$, 0.6 μL) were deposited on the walls of test tubes by evaporation of chloroform under argon. The films were rehydrated in PBS (1×, ∼0.01 M, 40 min) and subsequently subjected to eight freeze−thaw cycles (frozen in liquid nitrogen and thawed in warm tap water) and sonicated with a probe tip sonicator (Branson, 50% duty cycle for 5 min).

Waveguides and coverslips were assembled into a flow cell using a gasket to form a tight seal between them as has been outlined earlier (*5*−*7*). A supported bilayer was then formed on the cleaned flow cell surface by injecting the vesicle solution into the flow cell and allowing it to stabilize overnight. It is important to ensure that there are no air bubbles generated during the coating as they can damage the PLBs. The functionalized surface was subsequently blocked with PBS containing 2% BSA for 1 h before use for most experiments. These bilayer-coated waveguides remained stable for a maximum of 1 week under refrigeration.

Preparation of SAMs has also been described previously (*8*). Briefly, waveguide and coverslip surfaces were cleaned as described above. The substrates were submerged in water, blown dry, and placed in a vacuum desiccator with a small volume (∼50 μL) of 1-(3-aminopropyl)-1-methyldiethoxy silane (AP-MDES). The vacuum chamber was evacuated to ∼200 Torr and allowed to stand for 2 h. After coating, the substrates were baked at 110 °C for 30 min, allowed to cool in a drying desiccator, rinsed with ethanol, blown dry, and analyzed by contact angle. Poly(ethylene glycol) (PEG) reagents containing a carboxylic acid at one end and either a methoxy group (99−99.99% of the total PEG volume) or a protected amine (0.01−1% of the PEG volume) at the other were coupled to the amine surfaces overnight using standard peptide coupling conditions, again followed by contact angle analysis. The protecting groups were removed by immersion in a piperidine/NMP solution, and biotin was attached to the resulting free amine via its commercially available *N*-hydroxysuccinimide ester. All steps after aminosilanization were carried out in *N*-methylpyrrolidinone (NMP) as the solvent, and the slides were rinsed thoroughly between steps. After biotinylation, the slides were rinsed with NMP, acetone, and ethanol and were blown dry under a stream of argon. SAM-coated waveguides and coverslips were mounted into flow cells as described for the preparation and use of phospholipid bilayers, but the SAMs were not blocked and were therefore available for immediate use.

Waveguide-Based Sandwich Immunoassay for CEA. All experiments used the same batch of waveguides, functionalized and mounted in flow cells as described before. However, intrinsic waveguide background can vary, which accounts for some differences in the measured signal/background (S/B) (see Results).

A general schematic of the assay on the waveguide-based biosensor is shown in Figure 1 (unpublished data) (*6*). To provide a facile method of coupling light, diffraction gratings are etched on the surface of the waveguide. Excitation light is coupled into these gratings by positioning the laser beam at the appropriate angle of impingement. Two different excitation lasers were used: 532 nm (diode pumped Neodinium YAG laser, CrystaLaser, Reno, Nevada) for all QD experiments and 635 nm (Diode Laser, Coherent, Auburn, CA) for AF647 experiments. We selected waveguides that couple in approximately the same laser power (∼50% of the incident beam). A USB 2000 fiberoptic spectrometer (Ocean Optics, Dunedin) was used to collect isotropic emissions from the waveguide. Appropriate long-pass optical filters were used to filter out the excitation light. It is important to note that these filters do not affect the specific signal or alter the ratio of observed intensities.

All experiments used 100 nM each of the capture and detector antibodies and PBS-0.5% BSA as the wash buffer, with an injection volume of 200 μL. The flow cells were incubated for 5 min at room temperature and rinsed with approximately 20 flow cell volumes of buffer before measurement (3 s integration) unless otherwise specified. The following experimental groups were assessed: (1) SAMs vs PLBs as the functional surface for detection of CEA using T84.66-NH-AF647; (2) detection of CEA using T84.66-H-AF647 detector antibody; (3) detection of CEA using T84.66-NH-QD655 detector antibody; (4) detection of CEA using T84.66-H-QD655 detector antibody. All experiments were repeated at least twice using SAMs with 1% biotin except experiment 1.

The general experimental design is outlined in Figure 1. The first measurement acquired is the waveguide background, which quantifies a determination of the background fluorescence associated with intrinsic impurities in the waveguide surface.

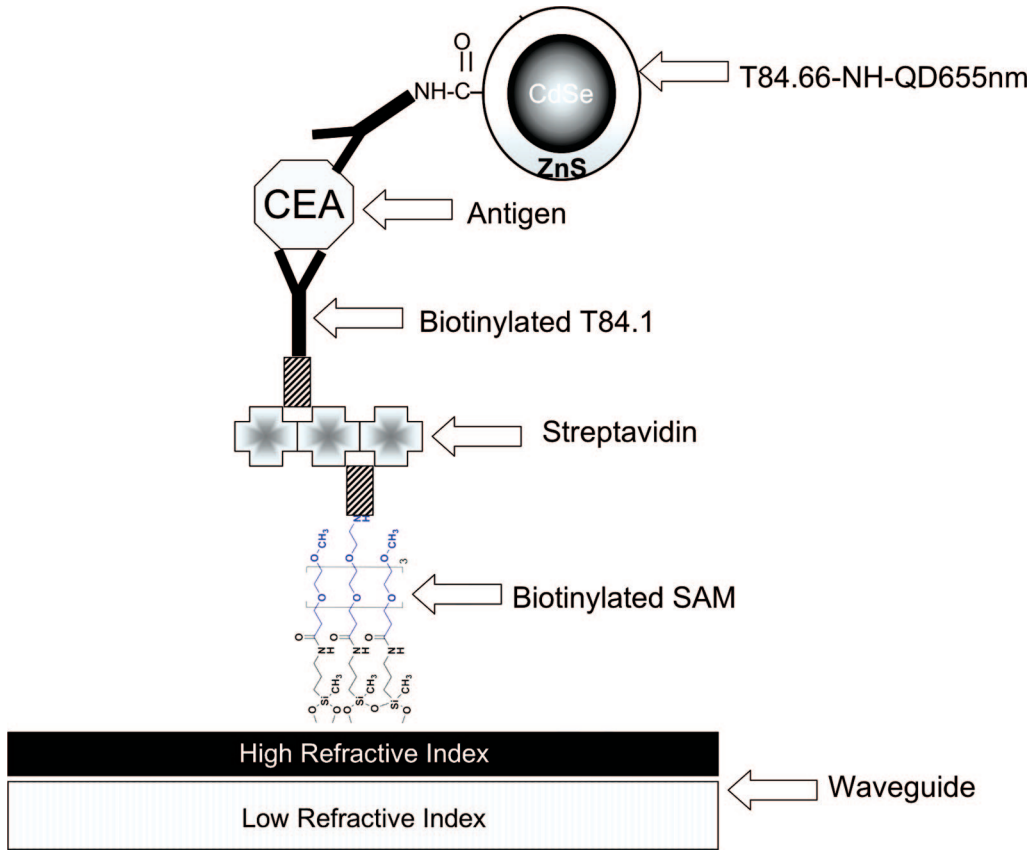

Figure 1. Schematic representation of the sandwich assay for CEA on a functionalized waveguide surface. Surface is functionalized with SAMs containing 1% biotin. Alternatively, PLBs can be used. This illustration depicts a detector antibody labeled with the QD in the NH domain. Both QDs and AF647 have been used for fluorescent labeling. Antibodies can be labeled in the NH domain or in the hinge region. See text for details. Diagram not to scale.

The assay utilizes the well-known biotin−avidin interaction to trap the biotinylated capture antibody to the waveguide surface. For this, the biotin on the PLB or SAM surface is entirely saturated with streptavidin (10 nM). A small concentration of streptavidin (1 pM) is fluorescently labeled with an organic dye (AF647 or 565 depending on the excitation wavelength used). The fluorescent signal (∼200−400 RFU) obtained from this is used as an indicator of system and surface functionality. Fluorescence measurements are relative to the instrument being used. The units reported in this manuscript are as measured on our waveguide-based optical biosensor using an Ocean Optics Spectrometer interface. Fluorescence measurements made using our biosensor will be reported as RFU in this manuscript. This signal is completely removed by repeat excitation with the laser (photobleaching, 15 s) before addition of the capture antibody to avoid skewing the results. Once the capture antibody is trapped, NSB associated with complex fluids is assessed by measuring the autofluorescence of a 50% solution of bovine serum in PBS. Next, the NSB of the fluorescent detector (the fluorescently labeled antibody used that particular experiment) is determined. This measurement is an indication of the nonspecific interaction of the fluorescent detector with the active surface in the absence of the antigen. The NSB signal is completely removed by photobleaching for the organic dyes before specific measurement is made. In the case of photostable QDs, the signal is subtracted from the final specific signal. In either case, repeat additions of the detector to the active surface are made (data not shown) to determine that there is no further increase in NSB.

Assessment of NSB is followed by antigen addition (CEA, 100 pM, 200 μL in PBS with 0.5% BSA). Following antigen incubation and wash, the detector antibody (100 nM, 200 μL in PBS) is added. Specific binding of the detector to CEA (effective sandwich) results in a positive signal, which is measured. Repeat excitations are performed to measure photostability.

RESULTS

CEA Detection Using T84.66-NH-AF647 Detector Antibody on a SAM vs PLBs. Figure 2A demonstrates detection of CEA (100 pM, 200 μL) on a SAM surface without any blocking. A signal of 3636 RFU over a waveguide background of 8 results in a S/B of 483. The NSB associated with 50% serum is 69 RFU, whereas that associated with the detector antibody is 193. In contrast, the S/B for the same assay using a PLB surface without blocking (Figure 2B) is only 44 (specific signal of 1143 over a background of 26 RFU). Some of the difference in measured S/B is attributed to the lower intrinsic background of some waveguides compared to the others. Yet, the NSB associated with serum (115 RFU) and the fluorescent detector (238 RFU) are also higher than that seen with SAMs, and the specific signal is greatly compromised with the use of PLBs. Assay performance on PLBs is dramatically improved when the defect sites in the bilayer that presumably give rise to NSB are preblocked with PBS containing 2% BSA for 2 h before use (Figure 2C). A S/B of 74 is realized (specific signal of 3030 RFU over a background of 41 RFU). When the PLBs are blocked, NSB associated with serum and detector antibody are both lower than seen in the absence of blocking, which is consistent with our previous results against other targets (*5, 7*). However, the assay performance is still poorer than that achieved with the use of SAMs.

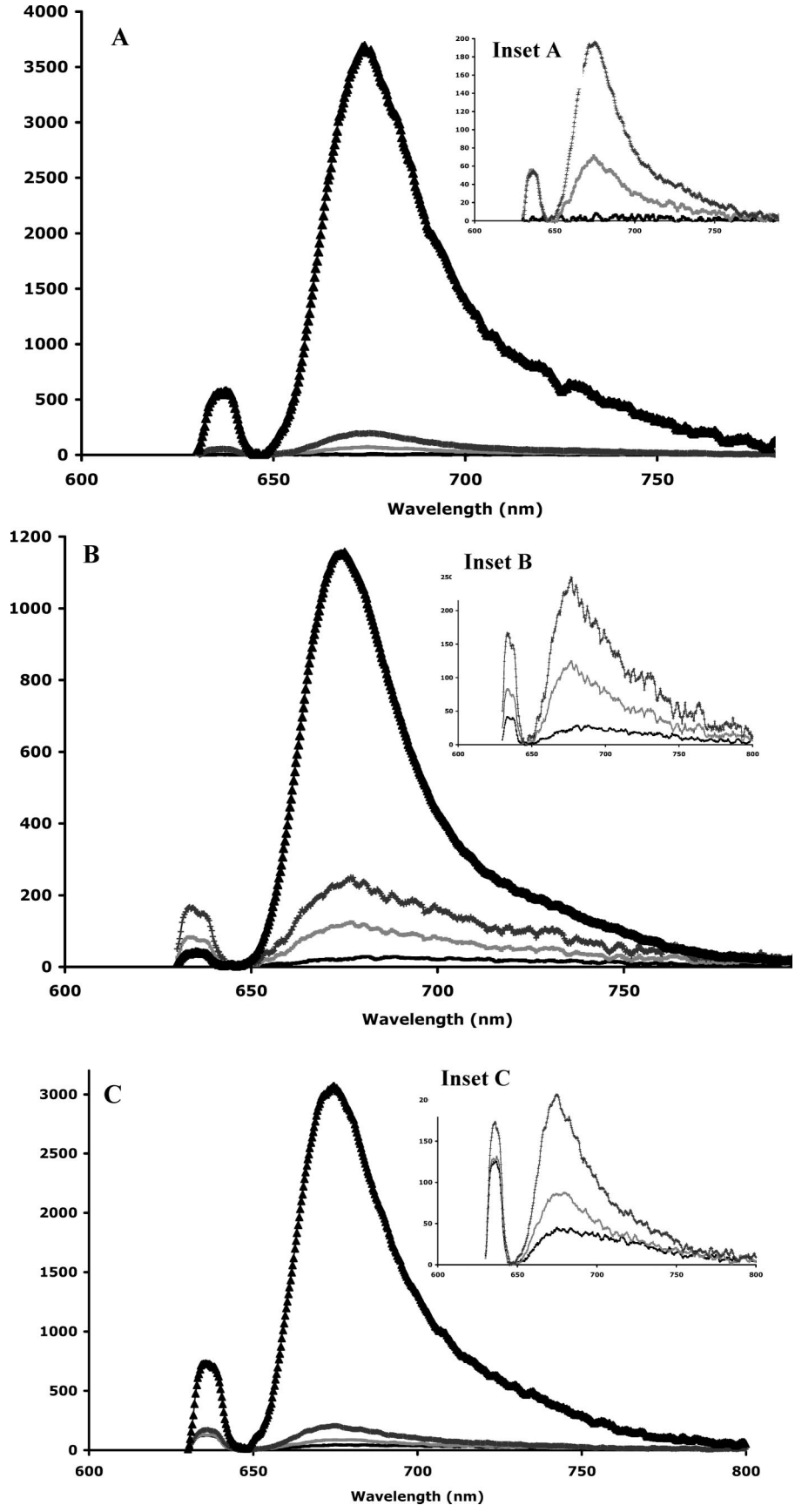

Figure 2. Determination of optimal surface for waveguide functionalization. CEA [100 pM] detection using T84.66-nH-AF647 detector antibody on a (A) SAM surface with 1% biotin, (B) PLB with 1% biotin without blocking, and (C) PLB with 1% biotin and blocking with PBS containing 2% BSA. Data are plotted as relative fluorescence units as a function of wavelength. Assay performance on a SAM surface (A) gives the maximal signal/background (483) and lowest NSB (69 RFU) for 100 pM CEA. Insets (in each graph) are an enlarged representation of the waveguide background and nonspecific binding curves redrawn for clarity. Key: Boxed squares (■) indicate waveguide background, gray circles (•) indicate nonspecific background associated with serum. + indicates detector associated nonspecific binding. Black triangles (▲) indicate specific signal with the addition of 100 pM CEA.

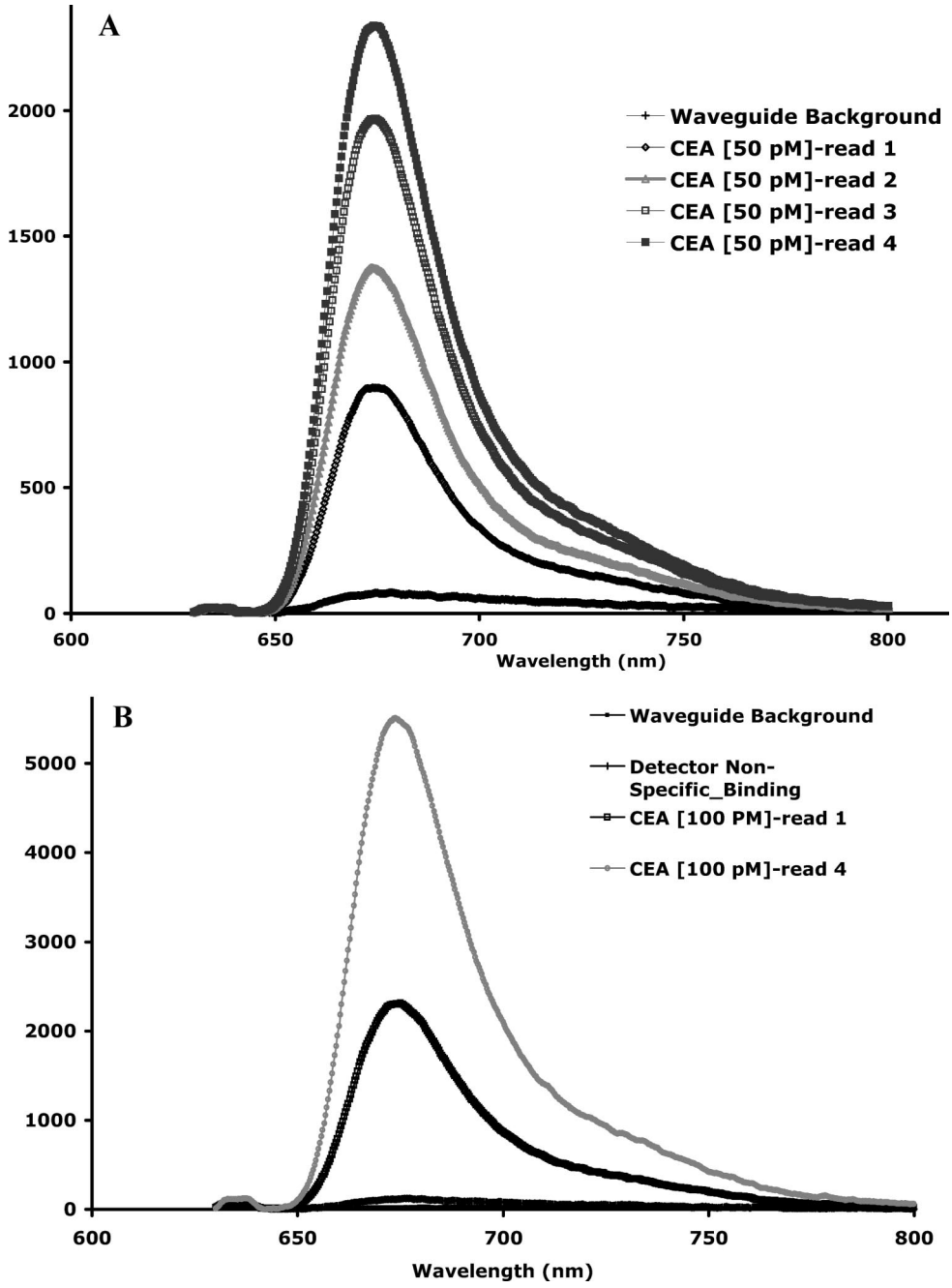

Figure 3. Unusual signal amplification using T84.66-H-AF647. Hinge labeling of the detector antibody with AF647 resulted in unusual signal amplification with repeat excitation (A). The amplitude of the measured signal almost doubled (over an unchanged background) after 4 repeat excitations. Figurer 3B demonstrates the initial (read 1, S/B of ~11) and final (read 4, S/B of 82) signals observed with [100 pM] CEA using this detector antibody.

Table 1. Summary of Measured Signal Intensity at Different Concentrations of CEA Using the Waveguide-Based Optical Biosensor[a]

[CEA] pM	signal (3 s) (RFU)	max signal (RFU)	integration time (s)	S/B (3 s)	S/B (12 s)
Bg	31.97 ± 8				
NSB	75 ± 14				
1	118.27	154.87	6	3.7	4.8
50	1212.6	2767.8	12	37.9	86.6
100	2302.72	5474.85	12	72.0	171.2
200	3033.08	6033.08	18	94.9	188.7

[a] T84.66-H-AF647 was used as the detector antibody.

Unusual Signal Amplification using T84.66-H-AF647 as the Detector. Hinge labeling of the detector antibody resulted in unusual signal amplification with repeat excitation (3 s integration each, Figure 3). Figure 3A demonstrates this increase in signal amplitude with repeat excitation in the detection of 50 pM CEA using T84.66-H-AF647. The initial signal (read 1) measured is 893 RFU over a waveguide background of 80 RFU, resulting in a S/B of 11.2. The amplitude of the measured signal increases to 1365 RFU (read 2) with repeat excitation corresponding to a S/B of 17 for the same concentration of CEA. The maximum signal measured for 50 pM CEA in this labeling format is 2320 RFU (read 4) resulting in a S/B of 29. Subsequent excitation results in photobleaching (data not shown). The exact reasons for this response are unclear but potential explanations are outlined in the Discussion. Figure 3B demonstrates signal obtained during the detection of CEA (100 pM) using this labeling strategy. An "initial" signal of 2303 RFU (read 1) over a waveguide background of 28 RFU corresponds to a S/B of

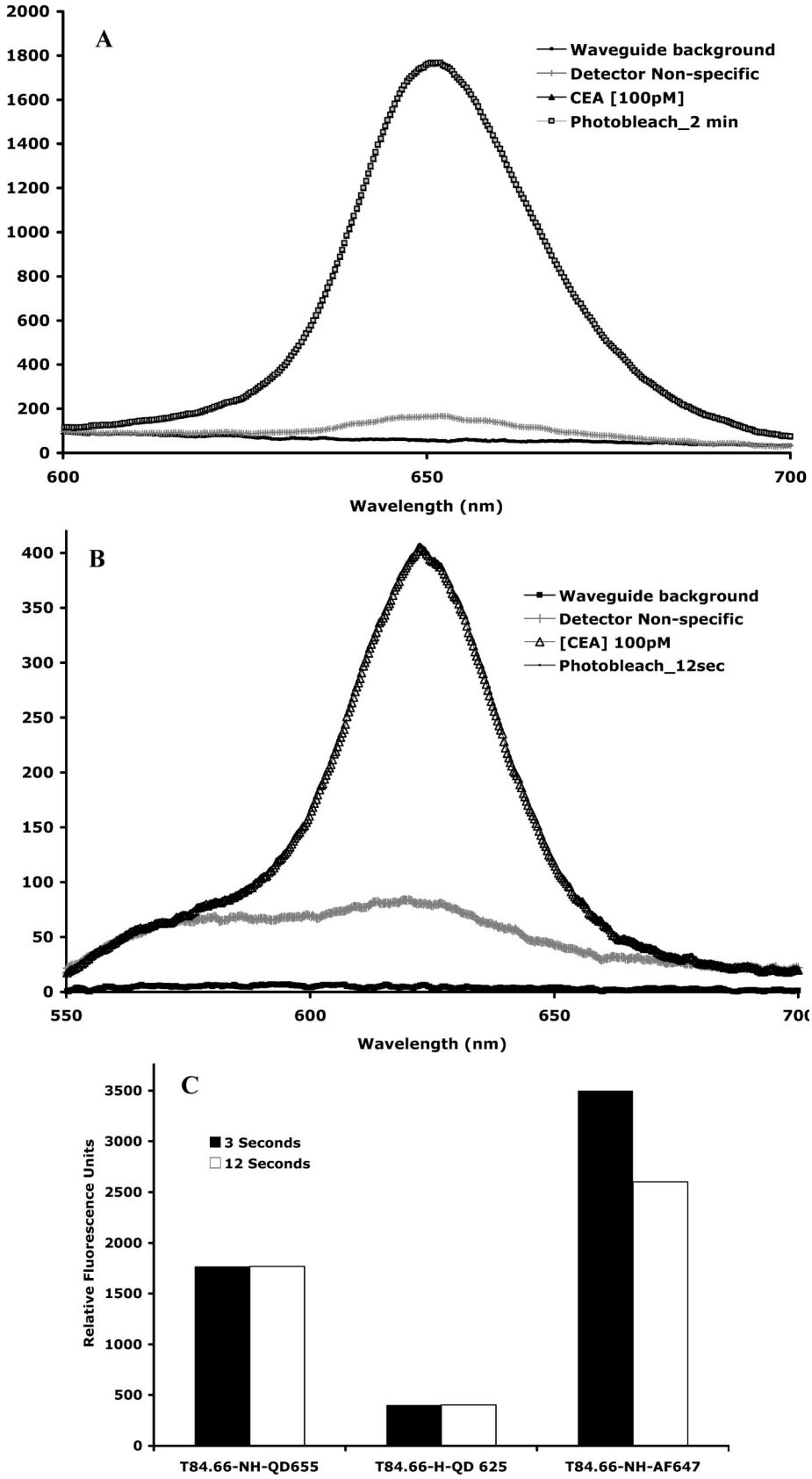

Figure 4. Detection of CEA using QD labeled antibodies. Both NH (QD655, A) and hinge (QD625, B) labeled antibodies were evaluated for the detection of 100 pM CEA. Whereas observed S/B is lower compared to that reported in Figure 2A, there is no photobleaching of the observed fluorescence after 2 min of excitation with the laser (C). As indicated in part C, the signal remains stable following 3 and 12 s of exposure to the laser when the antibody is labeled with QDs, whereas a significant decrease in intensity is seen when the antibody is labeled with AF647. Key: Boxed squares (■) indicate waveguide background, gray circles (•) indicate photobleaching after 12 s of exposure. + indicates detector associated nonspecific binding. Black triangles (▲) indicate specific signal with the addition of 100 pM CEA.

82, which is similar to that obtained with T84.66-NH-AF647 detector (Figure 2C, curve 1) for the same concentration of CEA. Repeat excitation resulted in increase in signal and a maximum signal intensity of 5498 RFU (read 4, S/B of 195), which is much higher than was observed with T84.66-NH-AF647 under similar experimental conditions. There is no increase in the detector antibody associated NSB with repeat excitation (6 repeats, 100 nM antibody in each addition, data not shown).

Table 1 summarizes signal amplification at different concentrations of CEA. The data was obtained from different waveguides, which explains the lack of absolute linearity in measured signals. The waveguide background and NSB values are averages of those obtained in the different experiments (all numbers were within the expected range). Repeat excitation of the fluorescent detector results in signal amplification in each case. Note that the excitation time required to achieve maximum signal is dependent on antigen concentration. Whereas the signal maximizes in 6 s with 1 pM CEA, it takes 18 s of excitation with 200 pM CEA. After the maximum signal is reached, photobleaching commences in each case. Thus, the maximum S/B obtained with any given concentration of CEA is significantly increased using this labeling strategy. Because the number of excitations required is dependent on the CEA concentration, it is difficult to use this approach for quantitative detection in unknown samples. However, this strategy could be advantageous in a purely qualitative test.

Detection of CEA Using QD Labeled Antibodies. Both NH (655 nm QD) and hinge (625 nm QD) labeling of T84.66 with QDs were evaluated. Figure 4A shows the signal obtained for the detection of 100 pM of CEA using 100 nM of T84.66-NH-QD655. A signal intensity of 1767 RFU is observed over a NSB (associated with detector antibody) of 167 RFU. Upon correction for NSB, a S/B of 3 is obtained. There is no apparent photobleaching observed despite 2 min excitation with the laser (532 nm) followed by a single reading at 3 s integration. We also evaluated hinge labeling of the detector antibody (Figure 4B). The observed signal intensity (402) was much lower than that seen with the other labeling paradigms, but the NSB and waveguide background were also lower. When corrected for NSB, a S/B of ~55 is evidenced for this labeling strategy. Again, the observed signal was extremely photostable, and there was no decrease in signal intensity following a 2 min excitation. A comparison of initial signals and the signal after 12 s exposure is shown in Figure 4C. Up to 10 μM of free QDs does not contribute to any measurable signal (data not shown).

DISCUSSION

This study addresses the surface and antibody labeling strategies to improve our current test for CEA. Generally, biodetection using the optical biosensor requires functionalization of the waveguide with a surface that allows for conjugation of antibodies or other recognition ligands. We have previously demonstrated the use of PLBs for waveguide functionalization and sensitive detection of CEA (*6*) (unpublished data). These surfaces are composed of lipid molecules, which make up all biological membranes. These structures are responsible for the selective permeability of cells, a factor that contributes to the low NSB associated with their use in most in vitro studies. In addition, bilayers are inexpensive, easy to prepare, and are well-suited for ligand attachment. However, lipid bilayers are unsuitable for a point-of-care diagnostic setting because they cannot endure prolonged storage (>1 week), harsh environments such as elevated temperatures, or passage through an air−water interface. Furthermore, high concentrations of lipids or urea in some biological samples (such as urine) results in elevated NSB, which limits the successful application of PLBs to biodiagnostic approaches. To overcome these disadvantages, we utilized PEG-modified, silane-based thin films. These coatings facilitate covalent attachment and chemical flexibility, and minimize NSB. We have previously demonstrated the application of these surfaces to the sensitive detection of the *Bacillus anthracis* protective antigen. Alkane SAMs terminated with PEG groups have been used for minimizing NSB (*8*). Concurrent with these results, use of SAMs as the functional surface in our assay abrogates the necessity for blocking. As shown in Figure 2A,B, lack of blocking diminishes the signal resolution obtained with PLBs as the functional surface, but it does not adversely affect functionality of the SAMs (data not shown).

Antibodies labeled with fluorescent dyes are inherently more stable. Of such dyes, long wavelength dyes (such as AF647) have lower background fluorescence (*18*−*20*). Alexa Fluor dyes are suited for bioapplications because of their brightness, photostability, water solubility, and pH compatibility. AF647, in particular, shows relatively small change in the fluorescence spectra and intensity when conjugated to antibodies in contrast with other dyes such as Cy5 (*20, 22*). Following this reasoning, we selected AF647 for our experimental setup. As indicated in Figure 2, use of T84.66-NH-AF647 as the labeled reporter antibody results in a significant S/B with 100 pM of CEA. There is a 15−20% decrease in signal with repeat excitation (photobleaching) as is typically expected from such dyes.

We also explored labeling T84.66 with AF647 in the hinge region. Labeling in this area is advantageous, since it directs the modification away from the antigen-binding region. This can be especially critical for larger reporters such as QDs. Mild reduction allowed for the generation of two half-antibody fragments containing free sulfhydryl groups in the hinge region. The fluorescent dye was then conjugated to the hinge region. When used as the detector for CEA, however, this material resulted in unusual signal enhancement (rather than photobleaching) with repeat excitation. It has been demonstrated that AF647 is more photostable and resistant to fluorescence quenching (at optimal degree of labeling) upon protein conjugation (*20, 22*). But the novel signal increase reported here is unprecedented. This antibody had 4 mol of AF647 per mole of protein, which is an optimal degree of labeling, according to the manufacturer. We have separated the labeled antibody from free AlexaFluor dye by gel filtration. In any case, we have also tested NSB associated with free AF647 in our assay and found no increase in fluorescence (data not shown). We speculate that, since multiple AF647 molecules are associated with a single antibody, some dye molecules are excited only after the fluorescence associated with others is quenched. This phenomenon, in combination to the relative photostability of AF647 dyes, could result in an increase in fluorescence. These hypotheses may explain why the increase in fluorescence is proportional to the concentration of the antigen, and hence the concentration of detector antibody in the system. Why this does not occur with T84.66-NH-AF647 (which also has ~4 mol of the dye/mol of protein) is, however, unclear. A possible explanation involves the conformation of the antibody when labeled in the hinge region, which allows for fluorescence quenching and subsequent photon release. It is apparent that the unusual signal amplification allows for a better S/B with lower concentrations of the antigen. This feature may be advantageous in attempting to develop a point-of-care diagnostic for breast cancer, especially in low volume samples such as NAF. However, since the degree of excitation and extent of amplification are dependent on the antigen concentration, quantitation of this phenomenon is not easy. This is a disadvantage for cancer detection, because most tumor biomarkers are normally expressed in the body at basal concentrations, even without cancer present. Therefore, a test for cancer should be quantitative for accurate diagnosis. This labeling strategy does

have potential for applications where a yes/no answer is adequate, e.g., infectious diseases like tuberculosis.

No single biomarker is an accurate indicator of cancer. Therefore, an efficient diagnostic strategy should be able to detect multiple biomarkers in a single sample. To achieve this eventuality, we explored the use of QD labeled antibodies as a fluorescence detector in our assay system.

In this manuscript, we evaluated both NH and SH labeling of antibodies. Both strategies allowed for the detection of CEA at a concentration of 100 pM, although the S/B was lower than that seen with T84.66-NH-AF647. The signal intensity measured with hinge labeling (Figure 4B) is lower than that seen with primary NH labeling (Figure 4A). However, the NSB is also lower. Therefore, the extrapolated S/B is comparable in both labeling strategies. Also, the observed signal is stable for over 2 min of excitation with the laser (Figure 4), a time over which signal from AF647 would be almost entirely photobleached. This photostability of core−shell quantum dots is a distinct advantage for multiplex detection as well, especially in attempting to engineer a multichannel sensor for simultaneous detection. It is also possible to envision an internal photostable standard (in lieu of streptavidin-AF647) that is used for both system functionality assessment and quantitation of antigen in unknown samples (unpublished data) (*6*).

To conclude, we have improved a sandwich assay for CEA on our waveguide-based OB by incorporating better surfaces and photostable detectors. These modifications will enable our biosensor to function as a robust research tool to probe biological interactions or as a point-of-care diagnostic method to detect a variety of disease targets.

ACKNOWLEDGMENT

The authors thank Karen Grace, Sohee Jeong, and Jennifer Martinez at the Los Alamos National Laboratory for help with waveguide instrumentation and helpful suggestions. This work was supported, in part, by a Los Alamos National Laboratory directed research (LDRD) grant.

LITERATURE CITED

(1) www.mayoclinic.com/health/breast_self_exam/WO00026.

(2) Berlin, L. (2001) The missed breast cancer redux: Time for educating the public about the limitations of mammography? *AJR 176*, 1131–1134.

(3) Hoisington, L. A., Scherer, D. L., and Berger, K. L. (2007) Breast MR imaging: applications and pitfalls. *Radiol. Technol. 78* (5), 367–377.

(4) Duff, M. J. (2006) Serum tumor markers in breast cancer: are they of clinical value? *Clin Chem. 52*, 345–351.

(5) Martinez, J. S., Grace, W. K., Grace, K. M., Hartman, N., and Swanson, B. I. (2005) Pathogen detection using single mode planar optical waveguides. *J. Mater. Chem. 15*, 4639–4647.

(6) Mukundan, H., Holt, A., Martinez, J. M., Kubicek, J., Shively, J. E., and Swanson, B. I. Planar optical waveguides for detection of tumor biomarkers, *Sens. Actuators*, in revision, 2008.

(7) Kale, R., Mukundan, H., Price, D., Foster-Harris, J., Lewallen, D. M., Swanson, B. I., Schmidt, J. G., and Iyer, S. S. (2008) Detection of intact influenza viruses using biotinylated biantennary S-sialosides. *J. Am. Chem. Soc. 130* (26), 8169–8171.

(8) Anderson, A. S., Dattelbaum, A. M., Montano, G. A., Price, D., Schmidt, J., Martinez, J. M., Grace, W. K., Grace, K., and Swanson, B. I. (2008) Functional PEG-modified thin-films for biological detection. *Langmuir 24* (5), 2240–2247.

(9) Pinaud, F., Michalet, X., Bentolila, L. A., Tsay, J. M., Doose, S., Li, J. J., Iyer, G., and Weiss, S. (2006) Advances in fluorescence imaging with quantum dot bio-probes. *Biomaterials 27* (9), 1679–87.

(10) Alivisatos, A. P. (1996) Semiconductor clusters, nano crystals and quantum dots. *Science 271* (5251), 933–937.

(11) Michalet, X., Pinaud, F., Bentolila, L. A., Tsay, J., Doose, S., Li, J., Sundaresan, G., Wu, A. M., Gambhir, S. S., and Weiss, S. (2005) Quantum dots for live cells and *in vivo* imaging, diagnostics and beyond. *Science 307* (5709), 538–544.

(12) Medintz, I. L., Uyeda, H. T., Goldman, E. R., and Matoussi, H. (2005) QD bioconjugates for imaging, labeling and sensing. *Nat. Mater. 4* (6), 435–446.

(13) Gao, X., Yang, L., Petros, J. A., Marshall, F. F., Simons, J. W., and Nie, S. (2005) In vivo molecular and cellular imaging with quantum dots. *Curr. Opin. Biotechnol. 16* (1), 63–72.

(14) Murray, C. B., Norris, D. J., and Bawendi, M. G. (1993) Synthesis and characterization of nearly monodisperse CdE (E = sulfur, selenium, tellurium) semiconductor nanocrystallites. *J. Am. Chem. Soc. 115*, 8706–8710.

(15) Hines, M. A., and Guyot-Sionnest, P. (1996) Synthesis and characterization of strongly luminescing ZnS-capped CdSe nanocrystals. *Phys. Chem. 100*, 468–471.

(16) Mattoussi, H., Mauro, J. M., Goldman, E. R., Anderson, G. P., Sundar, V. C., Mikulec, F. V., and Bavendi, M. G. (2000) Self assembly of CdSe-ZnS quantum dot bioconjugates using an engineered recombinant protein. *J. Am. Chem. Soc. 122*, 12142–12150.

(17) Gunsalus, C., Barton, L. S., and Gruber, W. (1956) Biosynthesis and structure of lipoic acid derivatives. *J. Am. Chem. Soc. 78*, 1763.

(18) Flanagan, J. H., Jr., Khan, S. H., Menchen, S., Soper, S. A., and Hammer, R. P. (1997) Functionalized tricarbocyanine dyes as near-infrared fluorescent probes for biomolecules. *Bioconjugate Chem. 8* (5), 751–756.

(19) Haugland, R. P. (2002) *Handbook of Fluorescent Probes and Research Products*, Molecular Probes Inc., Eugene, OR.

(20) Berlier, J. E., Rothe, A., Buller, G., Bradford, J., Gray, D. R., Filanoski, B. J., Telford, W. G., Yue, S., Liu, J., Cheung, C. Y., Chang, W., Hirsch, J. D., Beechem, J. M., and Haugland, R. P. (2003) Quantitative Comparison of Long-wavelength Alexa Fluor Dyes to Cy Dyes: Fluorescence of the Dyes and Their Bioconjugates. *J. Histochem. Cytochem. 51* (12), 1699–1712.

(21) Randolph, J. B., and Waggoner, A. S. (1997) Stability, specificity and fluorescence brightness of multiply-labeled fluorescent DNA probes. *Nucleic Acids Res. 25* (14), 2923–2929.

(22) Gruber, H. J., Hahn, C. D., Kada, G., Riener, C. K., Harms, G. S., Ahrer, W., and Dax, T. G. (2000) Anomalous fluorescence enhancement of Cy3 and Cy3.5 versus anomalous fluorescence loss of Cy5 and Cy7 upon covalent linking to IgG and noncovalent binding to avidin. *Bioconjugate Chem. 11*, 696–704.

BC800283E